Talanta 111 (2013) 47–53

Contents lists available at SciVerse ScienceDirect

Talanta

journal homepage: www.elsevier.com/locate/talanta

Graphene–polyaniline nanocomposite based biosensor for detection of antimalarial drug artesunate in pharmaceutical formulation and biological fluids

Keisham Radhapyari [a], Prabhat Kotoky [a], Manash R. Das [b], Raju Khan [a,*]

[a] Analytical Chemistry Division, CSIR-North East Institute of Science & Technology, Jorhat 785006, Assam, India
[b] Materials Science Division, CSIR-North East Institute of Science & Technology, Jorhat 785006, Assam, India

ARTICLE INFO

Article history:
Received 11 January 2013
Received in revised form
7 March 2013
Accepted 8 March 2013
Available online 26 March 2013

Keywords:
Biosensors
Graphene oxide
Nanocomposite
Antimalarial drug artesunate
Electrochemical impedance spectroscopy

ABSTRACT

Bioactive electrode of dispersed graphene oxide in polyaniline composite was electrochemically fabricated onto indium tin oxide substrate for pharmaceutical application. Formations of nanocomposite graphene–polyaniline matrix with diameter 67.99 nm were observed with the use of scanning electron microscope and high resolution transmission electron microscope. Electrochemical interfacial properties and immobilization of enzyme onto the graphene–polyaniline electrode have been evaluated and confirmed with the use of Fourier transform infrared spectroscopic, cyclic voltammetry and electrochemical impedance spectroscopic techniques. The graphene–polyaniline–horseradish peroxidase biosensor was further used for sensing artesunate a potent antimalarial drug. The biosensor shows linearity of 0.05–0.40 ng mL^{-1} of artesunate with sensitivity of 0.15 μA ng mL^{-1}. The procedure was applied to the assay of the drug in dosage form, human serum, plasma and urine without matrix interference. The limits of detection for parenteral artesunate, human urine, human serum and human plasma were 0.012 ng mL^{-1}, 0.013 ng mL^{-1}, 0.014 ng mL^{-1} and 0.014 ng mL^{-1} respectively. The mean percentage recoveries obtained were in the range from 98.23% to 100.3% for parental drug, urine, serum and plasma samples. The resultant precision and accuracy as evidenced have shown a promising selectivity in their application.

1. Introduction

Malaria is one of the major public health problems of all the developing countries with 2.5 million cases of malaria being annually reported in Southeast Asia alone [1] while it accounts for about 200,000 deaths per year in the population below 70 years of age in India [2], including 120,000 annual death in the age group of 15–69 years. This figure is greater than the WHO estimates [3]. Much of this morbidity and mortality is due to the poor quality of the anti-malarial drugs which results in drug resistance in the patient and inadequate treatment of the disease. Around 7% of the drugs tested in India were found to be of poor quality with many of them being fake [4]. In 2002, WHO recommended a group of antimalarials consisting of artemisinin and its derivatives especially artesunate, artemether and dihydroartemisinin as antimalarial drugs. In the treatment of severe malaria, parenteral artesunate have shown promising results by reducing mortality rate in Southeast Asian patients by 35% compared to quinine [5]. Artesunate is widely used as an antimalarial drug due to its little toxicity to humans and its potent effect on malarial parasites resistant to conventional antimalarial drugs [6]. Parenteral artesunate has, as a result, now become the recommended treatment for severe malaria in Southeast Asia. Since approximately 40% of the world population is at risk of malaria [7]. Antimalarial drugs have become a particular favorite of counterfeiters [8]. In Southeast Asia, the recent and widespread appearance of counterfeit artesunate poses a serious health hazard. Therefore, a sensitive, selective, fast and portable method is required for detection and quantification of counterfeit drug artesunate.

In view of the importance of artesunate in the treatment of malaria, several methods have been developed for quantitative analysis of artesunate and its metabolites in biological fluids and pharmaceutical formulations, based on high-performance liquid chromatography (HPLC) [9–15], colorimetric [16] liquid chromatography–mass spectrometry (LC–MS) [17–20], spectroscopic methods [21,22], thin layer chromatography (TLC) [23] capillary electrophoresis [24] and electrochemical method [25,26]. A survey of available literature reveals that electrochemical techniques such as cyclic voltammetry (CV), differential pulse voltammetry (DPV), square wave voltammetry (SWV) and electrochemical impedance spectroscopy (EIS) have widely been applied for determination of certain pharmaceuticals [27–30]. Selectivity and sensitivity of techniques

* Corresponding author. Tel.: +91 376 2370806; fax: +91 376 2370011.
E-mail address: khan.raju@gmail.com (R. Khan).

0039-9140/$ - see front matter © 2013 Elsevier B.V. All rights reserved.
http://dx.doi.org/10.1016/j.talanta.2013.03.020

can be drastically improved by surface modification of the working electrode followed by immobilization of biomolecules viz. enzyme [31,32] DNA [33] antibodies [34,35] glutamate oxidase [36] etc.

In this context, the use of biosensors offers as a very promising tool. The interest in their application in the pharmaceutical, biomedical and environmental field has increased lately as a result of their simplicity, specificity, sensitivity and, as fast and cost-effective and repetitive measurements with miniaturized and portable devices. For the last two decades, conducting polymers have emerged as one of the most interesting materials for the fabrication of biosensors and electrochemical sensors [37]. Polyaniline (PANI) is considered one of the promising and unique conducting polymers with certain advantages viz. fabrication of gas sensors, biosensors and field emitters [38,39]. Furthermore, PANI is not only environmentally stable but also dramatically changeable in its electronic structure and physical properties in pro-activate state [40]. Since PANI is the most studied and commonly used conducting polymer, functionalization of PANI with fullerenes and carbon nanotubes (CNTs) provides a new class of carbon-based advanced materials. In spite of various applications and advantages of fullerene, it is difficult to disperse it in the polymer matrices because of its strong molecular aggregate and crystallites form. It is, therefore, difficult to prepare the fullerene-conducting polymer composites [41].

Recently, CNT-reinforced polymer composites have extensively been studied for their application as biomedical materials [42] due to their outstanding mechanical, electrical, and thermal properties. CNTs functionalized with conducting polymers are promising for the development of new classes of multifunctional advanced materials [43]. Conducting polymer composites containing graphene possess good thermo-electric conductivity and mechanical stiffness [44]. Energy efficiency of graphene makes them an ideal candidate for future electronics applications, especially at the nanoscale. Uses of CNT in next-wave microchips are considered the most promising short-term applications for graphene reinforced biocompatible materials [45]. Many groups have reported on the synthesis, properties and application of PANI–graphene oxide with improved electrochemical performance as super capacitor electrode [46], gravimetric capacitance and volumetric capacitance [47], facile method to construct a hierarchical nanocomposite using 1D and 2D nanocomponents [48], and electrical properties measured by a four-probe method [49], GrO/PANI nanotubes exhibit an higher electrical conductivity [50]. However, no work has been reported on synthesis, properties and application of polyaniline–graphene nanocomposites for pharmaceutical applications. In spite of the facts that graphene is the youngest carbon allotrope, the exploration of its chemistry is rapidly advancing. In this manuscript we propose a new approach to electrochemical preparation of inorganic–organic hybrid GrO/PANI nanocomposite probe followed by immobilization of horseradish peroxidase (HRP) enzyme for determination of the artesunate in pharmaceutical formulations and biological fluids. The validated developed methods are simple, selective, and sensitive with effective testing procedures which could provide an affordable and practical means of rapidly monitoring drug quality and in pharmacokinetic studies that will help in improving the quality of life and the outcome would be a better control of diseases, quality and safety of drugs and food, and the last but not the least, improvement in the quality of our environment.

2. Materials and methods

2.1. Reagents and materials

Artesunate (99% purity) was a gift from Centaur Pharmaceuticals, Mumbai, India. Parenteral artesunate labeled to contain 60 mg artesunate per bottle was obtained from commercial sources. HRP, aniline monomer (99.5%) of analytical grade, ITO coated glass plates and Graphite powder ($<20\ \mu m$) was procured from Sigma Aldrich (Germany). $AgNO_3$ (99.8%, Qualigens, India), $NaBH_4$ ($>99\%$, S.D. Fine, India), hydrochloric acid (Qualigens, India), H_2O_2 (30% (w/v), Qualigens, India), $KMnO_4$ ($>99\%$, NICE-Chemical, India) were of analytical grade. Serum, urine and plasma were provided by NEIST, Clinical Centre from healthy volunteers and a pool of these was used. Serum, urine and plasma were kept frozen at $-20\ ^\circ C$ until assay. After gentle thawing, the samples were spiked with appropriate concentrations of the drug. A stock solution of artesunate 6 mg mL^{-1} was prepared by direct dissolution in freshly prepared 0.05 M phosphate buffer solution (PBS) of pH 7.01 ± 0.1 for experimental investigations. Standard working solutions were prepared by appropriate dilutions of the stock solution. Phosphate buffer solutions of 200 mL capacity with ionic strength 0.05 M in the pH range 5.5–9.0 were prepared in deionized water (TKA Millipore water system) by adding appropriately measured amounts mono sodium dihydrogen phosphate, disodium mono hydrogen phosphate and adjusting with 1 M HCl and 0.1 M NaOH solution.

2.2. Instrumentation

Electrochemical measurements were made using Autolab Potentiostat/galvanostat (Eco Chemie, Netherlands) with NOVA software and potentiostat/galvanostat/ZRA (Gamry Reference 3000, United States of America) with Gamry Echem Analyst Software in which a working electrode was replaced with PANI/ITO, GrO/ITO, GrO/PANI/ITO, and GrO/PANI/HRP/ITO. Platinum wire and Ag/AgCl (3 M KCl) were used as counter and reference electrodes respectively. Fourier transform infrared (FT-IR) spectrophotometer (Spectrum 100 with software version CPU32) has been used to characterize GrO–PANI nanocomposite and its interaction with enzyme (HRP). The surface morphology of films was studied with the use of Scanning Electron Microscopy (JEOL-JSM-6390LV). The high resolution transmission electron microscopy (HRTEM) images were taken by a TECNAI-T 30 model instrument operated at an accelerating voltage of 300 kV.

2.3. Preparation of graphene oxide (GrO)

GrO was prepared following powder graphite method of Hummer and Offman [51–53].

2.4. Electrochemical polymerization of GrO–PANI nanocomposite film

The nanocomposites of GrO–PANI were prepared by electrochemical deposition of a mixture of HCl (1.0 M), aniline (0.2 M) and GrO (50 μL in deionized water) and thoroughly sonicated for 15 minutes and these were introduced in a three-electrode electrochemical cell of Autolab Potentiostat/Galvonostat (EcoChemie, Netherlands, Model 101 N). The cell consists of Ag/AgCl (3 M KCl) as reference, Pt wire as counter electrode and ITO glass plate (0.25 cm^2) as working electrode. The electro-polymerization was demonstrated at scan rate of 20 mV s^{-1} in the potential range from 2.0 V to 1.1 V. The GrO/PANI/ITO electrode was washed with distilled water to clean the untreated GrO–PANI.

2.5. Immobilization of HRP on GrO–PANI nanocomposite film

The bio-electrode for detection of artesunate was prepared by immobilizing HRP (1 mg mL^{-1} solution in phosphate buffer, pH 7.01) onto the GrO–PANI nanocomposites by adsorption technique (overnight dipping in a special assembled cell) using glutaraldehyde mediator as a cross linker and incubated at 4 °C overnight.

The conditions for the immobilization of the enzyme were selected based on prior studies [54,55]. The biosensors were rinsed with a buffer solution to remove loosely-bound material and preserved at 4 °C at pH 7.01 ± 0.1 phosphate buffer solution for further use.

2.6. Preparation of real samples

Parenteral artesunate (*Larinate*) labeled to contain 60 mg of artesunate was transferred to 10 mL volumetric flask and completed to volume with freshly prepared 0.05 M phosphate buffer solution (PBS) with pH 7.01 ± 0.1 to make a stock solution of 6 mg mL^{-1}. Human serum, urine and plasma samples, used for measurement, were centrifuged and diluted 10 times with the buffer solution. The standard addition method was used for analyzing the pharmaceutical samples and artesunate-spiked human serum, urine and plasma samples for the validation of the modified electrode.

3. Results and discussion

3.1. FT-IR study

FT-IR spectra (Fig. 1) of PANI, GrO–PANI, GrO–PANI–HRP films were obtained to characterize the chemical interactions between PANI, GrO and HRP. FT-IR spectra of PANI has a strong absorption band between 714 and 843 cm^{-1} due to presence of an aromatic ring and deformation of C–H vibrations (Fig. 1a).

In the spectra, bands between 1204 and 1343 cm^{-1} are associated with C–N stretching in aromatic amines. The peak at 1648 cm^{-1} is attributed to C=C stretching of benzenoid rings and quinoid rings. The strong peak at 2355 cm^{-1} is due to –N-N in diazonium salts. The IR bands from 2982 cm^{-1} to 3300 cm^{-1} correspond to N-H stretching with hydrogen-bonded amino groups and free

O–H stretching vibration. The C=O stretching of carboxyl groups and the C–O vibrations of epoxy groups in GrO (Fig. 1b) are indicated by the appearance of peaks at 1723 and 1231 cm^{-1}. The C–O stretching of alkoxy group (1159 cm^{-1}) and O–H stretch peak (3369 cm^{-1}) evidenced that several types of functional groups were indeed generated by oxidation [56]. Compared with GrO, several new peaks attributed to PANI appeared in the spectrum of GrO–PANI (Fig. 1c). The new peaks at 1580, 1479, 1305, and 814 cm^{-1} are attributed to the vibration of C=N, C=C, C=N, and C=H respectively [57,58]. The FTIR spectrum of GrO–PANI–HRP (Fig. 1d) film has shown the characteristics of amide bands at (1635 cm^{-1}), due to the stretching vibration of peptide C=O groups, and amide II band at (1587 cm^{-1}), which results from a combination of N–H in plane bending and C–N stretching of peptide groups. The appearance of peaks at 1635 cm^{-1} and 1587 cm^{-1} indicates confirmation of the immobilization of HRP on GrO–PANI matrix.

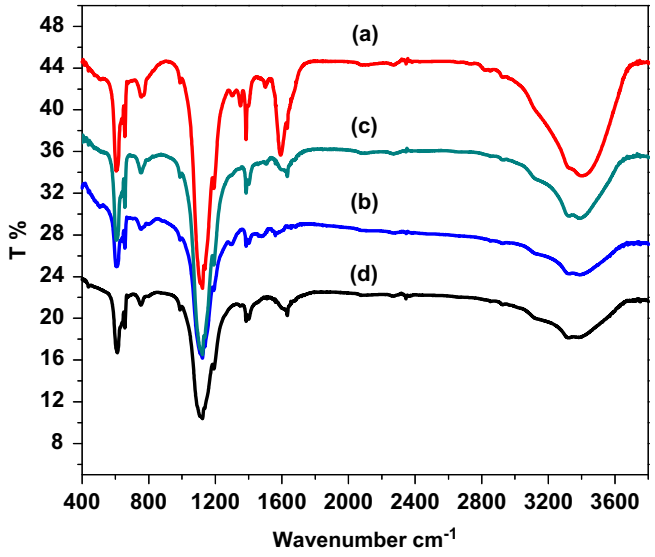

Fig. 1. FT-IR spectra of (a) PANI/ITO (b) GrO/ITO (c) GrO/PANI/ITO (d) GrO/PANI/HRP/ITO.

3.2. SEM and HRTEM studies

SEM and HRTEM micrographs were investigated to study the morphology of the electrodes surface.

Fig. 2(a) SEM of PANI film shows sponge like, rough structure. The morphology of the GrO was studied by HRTEM as shown in Fig. 2(b). It is observed from image that the GrO sheets are amorphous and disordered in nature and also forms multilayer agglomerates. SAED as shown in the inset of Fig. 2(b) observed the diffraction ring only with unresolved diffraction dots. GrO/PANI/ITO surface in Fig. 2(c) consists of highly porous matrix embedded with graphene nanocomposite of around 67.99 nm. On the basis of this information and the earlier investigations using the same type of electrodes based carbon nanotubes [59,60], it can be concluded that graphene nanocomposite could provide a matrix for the successful immobilization of the enzyme [61]. Fig. 2(d) shows the decrease in porosity and surface area of nanocomposite film. This is indicative of the successful immobilization of HRP enzyme on the electrode surface. However, the presence of the nano-pores due to GrO/PANI nanocomposite significantly contributed to the increase in electrode roughness in the surface area and demonstrated effective sensitivity of the biosensor.

3.3. CV study

Fig. 3 shows various cyclic voltammograms obtained for (a) PANI, (b) GrO (c) GrO/PANI electrodes and (d) GrO/PANI/HRP bio-electrode in PBS (50 mM, pH 7.01, 0.9% NaCl) containing 5 mM $[Fe(CN)_6]^{3-/4-}$ recorded at different scan rates (5–35 mVs^{-1}). In Fig. 3(e) difference between cathodic (E_{pc}) and anodic peak (E_{pa}) shift ($\Delta E_p = E_{pa} - E_{pc}$) was calculated and the linear increased in ΔE_p value with square root of scan rate indicates the slow kinetics of electron transfer on the electrode surface [37]. The effect of pH on the peak current was investigated in the pH ranges from 5.5 to 9.0 in presence of 0.05 ng mL^{-1} artesunate. The plot of current versus pH shows in Fig. 3(f) that maximum peak current and good peak shape was obtained at pH 7.01 ± 0.1 of PBS. Therefore, in order to maximize the signals of the biosensors current, a phosphate buffer solution (pH 7.01 ± 0.1) was selected as the optimum solution for all further experiments.

Addition of GrO in electrochemical polymerization of PANI had reduced ΔE_p value relative to only PANI which is an indication of increase in number of electrons ($n\alpha 1/\Delta E_p$) involved in the reaction. In Fig. 4, the two-fold increase in the slope of GrO/PANI/HRP electrode as compared to GrO–PANI indicates that HRP may have absorbed some of the electrons involved in the reaction at higher scan rates due to slow kinetics of electron transfer. Fig. 4 also shows the relative variation in CV (a) PANI (b) GrO (c) GrO–PANI and (d) GrO–PANI–HRP electrodes at constant scan rate (5 mV s^{-1}) in PBS (50 mM, pH 7.01, 0.9% NaCl) containing 5 mM $[Fe(CN)_6]^{3-/4-}$ for three electrodes.

After addition of GrO into PANI, the slope of GrO–PANI has enhanced by a factor of about two. This enhancement of current might be related to hydrogen bonding of GrO (–OH, hydroxyl group) with PANI (–NH, amino group) as observed in FTIR. During the bio-electrochemical reaction, decrease in peak current in Fig. 4(d) is due to slow redox process after immobilization of HRP on GrO/PANI

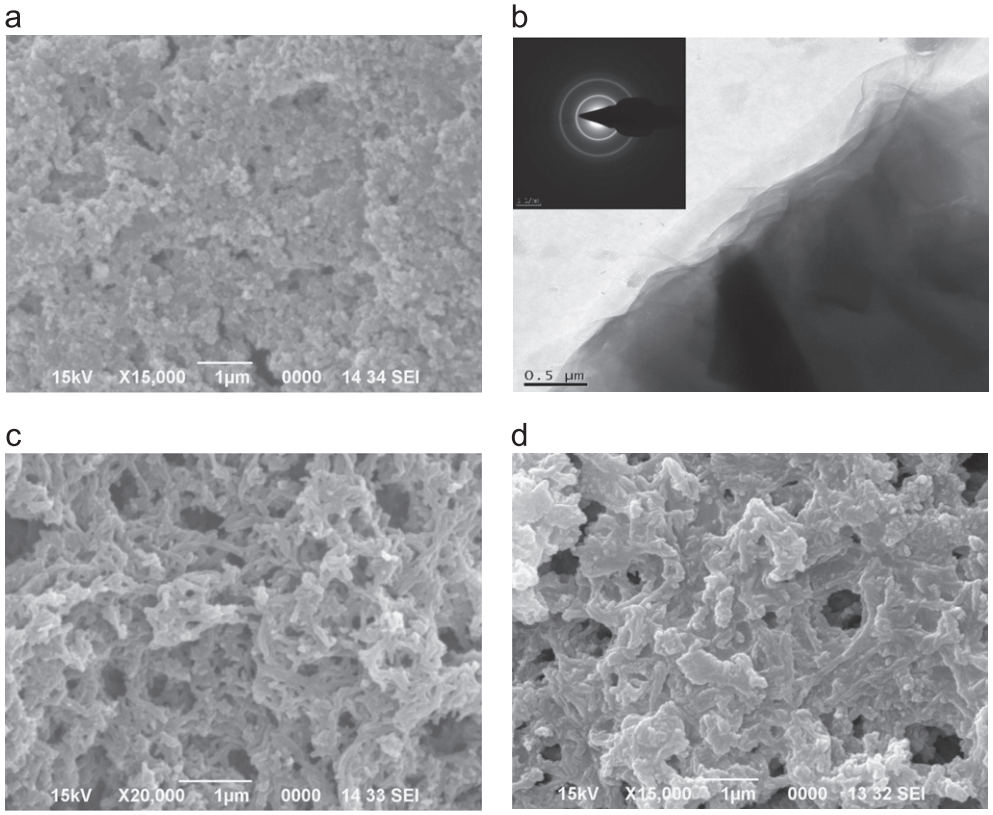

Fig. 2. SEM and HRTEM micrograph of the surface (a) PANI/ITO (b) HRTEM images of GrO matrix (c) GrO/PANI/ITO and (d) GrO/PANI/HRP/ITO electrodes.

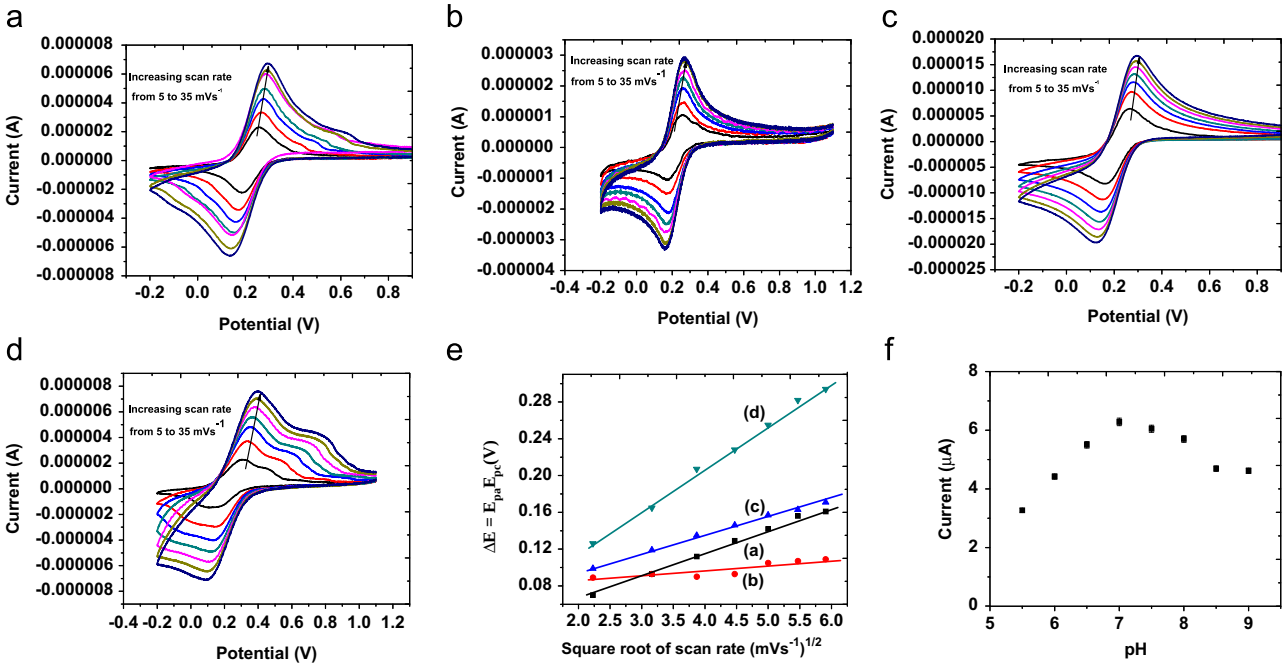

Fig. 3. Cyclic voltammograms of: (a) PANI/ITO, (b) GrO/ITO (c) GrO/PANI//ITO, and (d) GrO/PANI/HRP/ITO electrodes in PBS (50 mM, pH 7.0, 0.9% NaCl) containing (5 mM) $[Fe(CN)_6]^{3-/4-}$ at scan rate from 05 mV s^{-1} to 35 mV s^{-1}, (e) difference between cathodic (E_{pc}) and anodic peaks (E_{pa}) and (f) effect of pH on the amperometric response of the biosensor to artesunate.

electrode. All the three electrodes showed relative variation in the oxidation (I_{pa}) and reduction (I_{pc}) peak current against $\nu^{1/2}$ (ν is the scan rate). The peak current (I) is proportional to $n^{3/2}D^{1/2}\nu^{1/2}$ for constant surface areas and concentrations; whereas n and D are the number of electrons and diffusion coefficient, respectively. Intuitively, the current intensity (i.e. the flow of electrons) is expected to depend on the surface area of the working electrode and the concentration of the electro-active species. The surface concentration

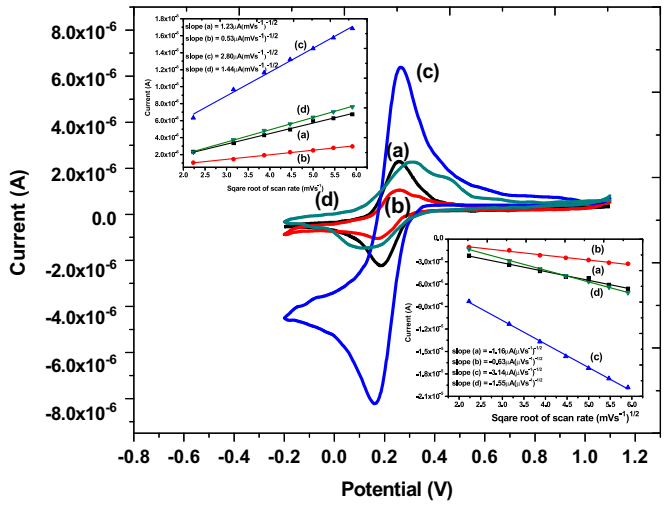

Fig. 4. Comparisons of the peak currents in cyclic voltammograms: (a) PANI/ITO, (b) GrO/ITO (c) GrO/PANI//ITO, and (d) GrO/PANI/HRP/ITO electrodes in PBS (50 mM, pH 7.0, 0.9% NaCl) containing (5 mM) $[Fe(CN)_6]^{3-/4-}$ scan rate at 10 mV s^{-1}. Picture in inset shows reduction and oxidation peak current with square root of scan rate.

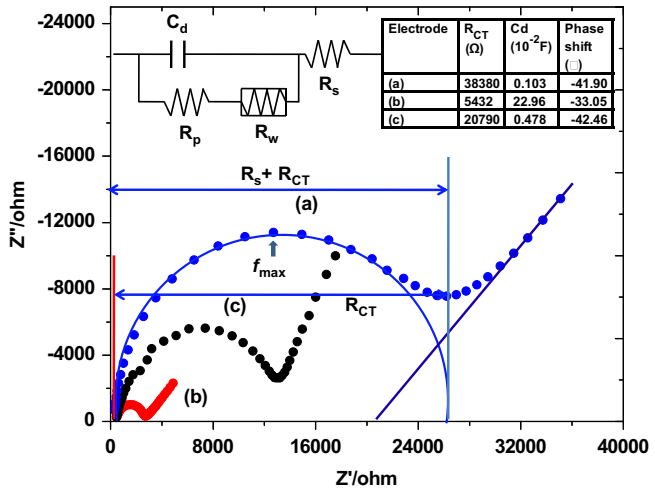

Electrode	R_{CT} (Ω)	Cd (10^{-2}F)	Phase shift (°)
(a)	38380	0.103	-41.90
(b)	5432	22.96	-33.05
(c)	20790	0.478	-42.46

Fig. 5. EIS Nyquist plots of PANI/ITO (b) GrO/PANI/ITO (C) GrO/PANI/HRP/ITO and picture in inset table shows R_{CT}, C_D and Phase Shift (Φ) values of PANI/ITO, GrO/PANI/ITO and GrO/PANI/HRP/ITO.

of the biosensor can be estimated from the plot of current versus potential using Brown-Anson Model [63]. The value of the surface concentration of the biosensor has been found to be 1.587×10^{-9} mol cm^2. Diffusion coefficient depends on the slope of peak current with square root of scan rate $[d(I)/d(\nu^{1/2})]$ is proportional to $D^{1/2}$, where linear response with the scan rate shows a diffusion controlled process. Diffusion process on the electrode surface was increased about five times due to addition of GrO. As it is pointed out above, the two-fold increase in slope in Fig. 4(c) as compared to Fig. 4a is due to the formation of hybrid GrO/PANI. The drastic decrease in slope in Fig. 4(d) was observed and is possibly due to strong binding of HRP to GrO–PANI matrix and control in transport of ions of the supporting electrolyte.

3.4. EIS study

EIS was carried out on PANI, GrO/PANI and GrO/PANI/HRP films (Fig. 5) to investigate the effect of surface charge modulation for determination of relative change in surface resistance at zero potential.

The electrochemical complex matrix (Z) can be represented as the sum of the real (Z') and imaginary ($-Z''$) components [$Z=Z'+j(-Z'')$, where $j=\sqrt{-1}$] that originate generally from the resistance and capacitance of an electrolytic cell. Nyquist plot of impedance was obtained at different frequencies and the equation of parallel RC circuit is as follows [62]:

$$Z(\omega) = Z' + jZ'' = R_s + R_p/(1+j\omega C_d) \quad (1)$$

$$Z' = R_s + R_p/1+\omega^2 R_p^2 C_d^2 \text{ and } -Z'' = \omega R_p^2 C_d/1+\omega^2 R_p^2 C_d^2 \quad (2)$$

where R_s is the electrolyte solution resistance and R_p is polarization resistance. R_{CT} is the surface charge transfer resistance as R_p obtained at zero potential and C_d is the double layer capacitance at the electrode/solution interface. The frequency associated with maximum Z'' and R_{CT} was used to calculate C_d using the following equation:

$$R_{CT}C_d = 1/2\pi f_{max} \quad (3)$$

From the generated data (inset table in Fig. 5), we notice a drastic decrease in the charge transfer resistance value in GrO/PANI electrodes and evidence of more conductivity. On the other hand, the calculated higher value of electrical double layer (C_d) in GrO/PANI interface is probably related to increase in the electrode surface. This increase in the capacitance and the higher value of C_d suggested the successful incorporation of GrO into the PANI films which is also supported by CV study (Fig. 4). An increase in the R_{CT} is observed on immobilization of HRP to GrO/PANI film. Furkan et al. [63] had successively demonstrated the use of electrochemical impedance spectroscopy for monitoring HRP hindrance of the molecular structure with a metal surface. Therefore, the change in R_{CT} after HRP immobilization was due to dielectric and insulating features at the electrodes electrolyte interface and was associated with successive immobilization of HRP.

3.5. Application to real samples

3.5.1. Pharmaceutical assay

The applicability of the proposed GrO–PANI nanocomposite based electrochemical biosensor on the sample dosage form was examined by analyzing parenteral artesunate (60 mg) shown in Fig. 6.

There was no need for filtration of injection extracts from undissolved excipients, just dilution of an aliquot with the supporting electrolyte (PBS, pH 7.01 ± 0.1) is required before measurement. The current is mainly diffusion controlled and proportional to the concentration over a convenient range. Fig. 6 (*in inset*) shows that under the optimized condition the linear relationship between the artesunate concentration and peak current is due to the generation of peak product hydrogen peroxide [64,65].

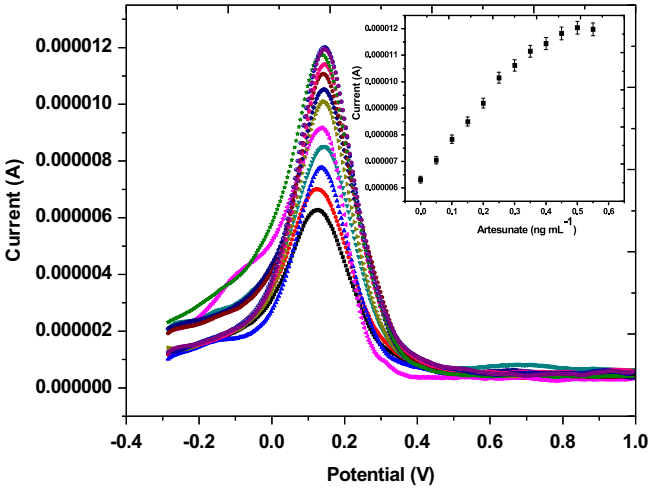

Fig. 6. Biosensors response with increases in concentration of artesunate and inset calibration curve shows linearity for artesunate as 0.05–0.40 ng mL^{-1}.

Table 1
Comparison of the different methods for artesunate determination.

Method	Detection limit/(Quantification limit)				Refs.
	Dosage form	Human urine	Human serum	Human plasma	
Non-biosensor					
HPLC-EC	–	–	–	8.0 ng mL^{-1}	[9]
HPLC-ELSD	8.0 mg mL^{-1}	–	–	–	[10]
HPLC-UV	52.35 μg mL^{-1}	–	–	–	[11]
HPLC-UV	–	–	–	8.0 ng mL^{-1}	[12]
HPLC-EC	–	–	–	5.0 ng mL^{-1}	[13]
HPLC-UV	87.97 μg mL^{-1}	–	–	–	[14]
HPLC-DAD	3.460 μg mL^{-1} (10.485 μg mL^{-1})	–	–	–	[15]
Colorimetric	0.250 mg mL^{-1}	–	–	–	[16]
LC–MS	–	–	–	0.5 ng mL^{-1}	[17,18]
LC–MS	–	–	–	0.5 ng mL^{-1} (1.5 ng mL^{-1})	[19]
LC–MS				25 ng mL^{-1}	[20]
Spectrofluorometric	0.471 mg mL^{-1}	–	–	–	[21]
Spectrophotometric	4.3 ng mL^{-1}	–	–	–	[22]
TLC	<1 μg mL^{-1}	–	–	–	[23]
Capillary electrophoresis	(330 mg L^{-1})	–	–	–	[24]
MWCNT/GCE	2.49 ng mL^{-1}	–	–	–	[25]
GCE in solubilized system	0.034 μg mL^{-1}	0.066 μg mL^{-1}	0.245 μg mL^{-1}	0.120 μg mL^{-1}	[26]
Biosensors					
GrO/PANI/HRP biosensor	0.012 ng mL^{-1}	0.022 ng mL^{-1}	0.016 ng mL^{-1}	0.0312 ng mL^{-1}	Present study

The amount of compound in the dosage form was calculated by standard addition method (Table 1). The accuracy and precision in results obtained for the parenteral artesunate was found to be in good agreement with that of the prescribed values of drug taken from formulations. The effect of excipients on the voltammetric response of artesunate was studied and it was shown that in the proposed method, co-administered drugs did not interfere. The analytical performance data of the proposed method are compiled (Table 2 supplement information). Statistical and performance characteristic of the analytical method from the calibration data is also shown (Table 3 supplement information). Recovery studies of the drug in pharmaceutical formulation (parenteral form) were performed using the standard addition method. The precision and accuracy of artesunate in parenteral form were assessed from five replicates at nominal concentration. The precision is expressed as the percentage relative standard deviation (%RSD), and accuracy is expressed as a mean percentage recoveries (%*R*) (Table 5 supplement information).

3.5.2. *Biological fluids assay*

The applicability of the proposed GrO/PANI/HRP/ITO bioelectrode based electrochemical biosensor is studied in spiked biological samples viz. human urine, serum and plasma. Calibration equation parameters and related validation data are shown in Table 2 supplement information. Recovery experiments were performed using the standard addition method. The obtained results are presented in Tables 4 and 5 supplement information showing significant recovery values in spiked human urine as (95.41%), spiked human serum (96.55%) and spiked human plasma (95.81%). Moreover, it has demonstrated considerable repeatability and reproducibility, along with accuracy and precision in experimental study and confirms as a promising alternative method for the direct determination of artesunate in pharmaceutical formulations and spiked biological fluids. The advantages in the form of a comparative study on results obtained from the present approach with already existing ones are presented in Table 1.

4. Conclusion

We have successfully developed a highly sensitive and selective, biosensor-based GrO/PANI/HRP nanocomposite probe for direct determination of artesunate in a pharmaceutical formulation and biological fluids. The present biosensor exhibits low detection limits and high levels of repeatability and reproducibility in a pharmaceutical formulation and biological fluids (urine, plasma and serum). These results strongly support our contention that electroanalysis can be used in the detection of artesunate and the strategy described here has many attractive advantages viz. simplicity, sensitivity, selectivity, rapidity, and low cost which will all act as great incentives for its use in the quality analysis of drugs, medicines, and other analytes of interest in the pharmaceutical area.

Acknowledgments

Dr. K. Radhapyari is grateful to the Department of Science and Technology (DST), Government of India, New Delhi for financial support awarded under Fast Track Young Scientist Project sanctioned vide No. SR/FTP/CS-104/2007. All authors are thankful to the Centaur Pharmaceuticals, Mumbai, India for providing the standards and to Dr. P.K. Baruah, Medical Officer, CSIR-NEIST Clinical Centre, Jorhat, India for providing urine, serum and plasma samples. We also extend our sincere thanks to Dr. B.S. Bhau, Senior Scientist, MAEP Division, CSIR-NEIST for his help in preparing the biological fluid (urine, serum and plasma) samples. We are also grateful to Dr. R.C. Boruah, Acting Director, CSIR-NEIST, Jorhat India for providing the laboratory facilities and for his kind permission to publish the paper. The authors thank Mr. Ratan Baruah Tezpur University, Tezpur, India for SEM measurements.

Appendix A. Supporting information

Supplementary data associated with this article can be found in the online version at http://dx.doi.org/10.1016/j.talanta.2013.03.020.

References

[1] A.P. Dash, N. Valecha, A.R. Anvikar, A. Kumar, J. Biosci. 33 (2008) 583–592.
[2] N. Dhingra, P. Jha, V.P. Sharma, A.A. Cohen, R.M. Jotkar, P.S. Rodriguez, D.G. Bassani, W. Suraweera, R. Laxminarayan, R. Peto, Lancet 376 (2010) 1768–1774.

[3] World Health Organization, World Malaria Report. WHO/HTM/GMP 2008.1. Geneva, Switzerland, 2008. Available at: ⟨http://www.who.int/malaria/wmr2008/⟩.
[4] S. Kounteya, 7% of Malaria Drugs in India Fake: Study. Times News Network, 2012. Available at: ⟨http://articles.timesofindia.indiatimes.com/2012/may/22⟩.
[5] A. Dondorp, F. Nosten, K. Stepniewska, N. Day, N. White, Lancet 366 (2005) 717–725.
[6] T.T. Hein, N.J. White, Lancet 341 (1993) 603–608.
[7] World Health Organization, Fact Sheet 94. Revised October 1998. Available at: ⟨http://www.who.int/mediacentre/factsheet/fs94/en/⟩ (accessed 01.06).
[8] A. Dondorp, P. Newton, M. Mayxay, W. Van Damme, F. Smithuis, S. Yeung, Trop. Med. Int. Health 9 (2004) 1241–1246.
[9] Choon-Sheen Lai, N.K. Nair, A. Muniandya, S.M. Mansora, P.L. Olliarob, V. Navaratnam, J. Chromatogr. B 877 (2009) 558–562.
[10] K. Gaudin, T. Kauss, Anne-Marie Lagueny, P. Millet, F. Fawaz, Jean-Pierre Dubost, J. Sep. Sci. 32 (2009) 231–237.
[11] S.S. Ranher, S.V. Gandhi, S.S. Kadukar, P.N. Ranjane, J. Anal. Chem. 65 (2010) 507–510.
[12] Choon-Sheen Lai, N.K. Nair, S.M. Mansor, P.L. Olliaro, V. Navaratnam, J. Chromatogr. B 857 (2007) 308–314.
[13] K. Na-Bangchang, K. Congpuong, L.N. Hung, P. Molunto, J. Karbwang, J. Chromatogr. B 708 (1998) 201–207.
[14] S. Gandhi, P. Deshpande, P. Jagdale, V. Godbole, J. Chem. Pharm. Res. 2 (2010) 429–434.
[15] M.U. Phadke, V.K. Jadhav, R.K. Jadhav, S.S. Dave, D.S. Patil, Chromatographia 68 (2008) 1003–1007.
[16] M.D. Green, D.L. Mount, R.A. Wirtz, N.J. White, J. Pharm. Biomed. Anal. 24 (2000) 65–70.
[17] W. Hanpithakpong, B. Kamanikom, A.M. Dondorpa, P. Singhasivanon, N.J. Whitea, N.P.J. Daya, N. Lindegardh, J. Chromatogr. B 876 (2008) 61–68.
[18] N. Lindegardh, A.M. Dondorp, P. Singhasivanon, N.J. White, N.P.J. Day, J. Pharm. Biomed. Anal. 45 (2007) 149–153.
[19] E.M. Hodel, B. Zanolari, T. Mercier, J. Biollaz, J. Keiser, P. Olliaro, B. Genton, L.A. Decosterd, J. Chromatogr. B 877 (2009) 867–886.
[20] S.A.A. Van Quekelberghe, S.A Soomro, J.A. Cordonnier, F.H. Jansen, J. Anal. Toxicol. 32 (2008) 133–139.
[21] T.V. Sreevidya, B. Narayana, Eurasian J. Anal. Chem. 4 (2009) 119–126.
[22] C.O. Esimone, E.O. Omeje, F.B.C. Okoye, W.O. Obonga, B.U. Onah, J. Vector Borne Dis. 45 (2008) 281–286.
[23] Jean-Robert Ioset, H. Kaur, PLoS ONE 4 (2009) 1–8.
[24] N.C. Amin, M.D. Blanchin, M. Aké, J. Montels, H. Fabre, Malar. J. 11 (2012) 149.
[25] R. Jain Vikas, Chem. Sensors 15 (2011) 1–8.
[26] R. Jain Vikas, Colloids Surf. B: Biointerface 88 (2011) 729–733.
[27] V.K. Gupta, R. Jain, K. Radhapyari, N. Jadon, S. Agarwal, Anal. Biochem. 408 (2011) 179–196.
[28] R. Jain, K. Radhapyari, N. Jadon, J. Electrochem. Soc. 155 (2008) F104–F109.
[29] R. Jain, V.K. Gupta, N. Jadon, K. Radhapyari, J. Electroanal. Chem. 648 (2010) 20–27.
[30] R. Khan, M. Dhayal, Electrochem. Commun. 10 (2008) 263–267.
[31] R. Khan, A. Kaushik, P.R. Solanki, A.A. Ansari, M.K. Pandey, B.D. Malhotra, Anal. Chim. Acta 616 (2008) 207–213.
[32] R.A. Olowu, O. Arotiba, S.N. Mailu, T.T. Waryo, P. Baker, E. Iwuoha, Sensors 10 (2010) 9872–9890.
[33] Jin-Young Park, Su-Moon Park, Sensors 9 (2009) 9513–9532.
[34] R. Khan, M. Dhayal, Biosen. Bioelectron. 24 (2009) 1700–1705.
[35] R. Khan, N.C. Dey, A.K. Hazarika, K.K. Saini, M. Dhayal, Anal. Biochem. 410 (2011) 185–190.
[36] R. Khan, W. Gorski, C.D. Garcia, Electroanalysis 23 (2011) 2357–2363.
[37] A.K. Mulchandani, C.L. Wang, Electroanalysis 8 (1996) 414–419.
[38] S. Virji, J. Huang, R.B. Kaner, B.H Weiller, Nano Lett. 4 (2004) 591–596.
[39] Y. Shen, Y. Lin, C.W. Nan, Adv. Funct. Mater. 17 (2007) 2405–2410.
[40] P.J. Kinlen, J. Liu, Macromolecules 31 (1998) 1735–1744.
[41] I. Yu Sapurina, J. Stejskal, M. Trchová, D. Hlavatá, F. Biryulin Yu, Nanostructures 14 (2006) 447–455.
[42] X.F. Shi, B. Sitharaman, Q.P. Pham, F. Liang, K. Wu, W.E. Billups, L.J. Wilson, A.G. Mikos, Biomaterials 28 (2007) 4078–4090.
[43] S. Shaikh, K. Lafdi, E. Silverman, Carbon 45 (2007) 695–703.
[44] S. Stankovich, D.A. Dikin, G.H.B. Dommett, K.M. Kohlhaas, E.J. Zimney, E.A. Stach, R.D. Piner, S.T. Nguyen, R.S. Ruoff, Nature 442 (2006) 282–286.
[45] M.A. Rafiee, J. Rafiee, Z. Wang, H.H. Song, Z.Z. Yu, N. Koratkar, ACS NANO 3 (2009) 3884–3890.
[46] H. Wang, Q. Hao, X. Yang, L. Lu, X. Wang, Appl. Mater. Interfaces 2 (2010) 821–828.
[47] D.W. Wang, F. Li, J. Zhao, W. Ren, Z.G. Chen, J. Tan, Z.S. Wu, I. Gentle, G. Qing Lu, H.M. Cheng, ACS NANO 3 (2009) 1745–1752.
[48] J. Xu, K. Wang, S.Z. Zu, B.H. Han, Z. Wei, ACS NANO 9 (2010) 5019–5026.
[49] N. Yang, J. Zhai, M. Wan, D. Wang, L. Jiang, Synth. Met. 160 (2010) 1617–1622.
[50] Y.F. Huang, C.W. Lin, Polymer 53 (2012) 1079–1085.
[51] W.S. Hummers, R.E. Offeman, J. Am. Chem. Soc. 80 (1958) 1339 1339.
[52] O. Fellahi, M.R. Das, Y. Coffinier, S. Szunerits, T. Hadjersi, M. Maamache, R. Boukherroub, Nanoscale 3 (2011) 4662–4669.
[53] M.R. Das, R.K. Sarma, R. Saikia, V.S. Kale, M.V. Shelke, P. Sengupta, Colloids Surf. B: Biointerface 83 (2011) 16–22.
[54] Y. Wang, Zi Shi, Yin Jie Xing, Polymer 52 (2011) 3661–3670.
[55] A.P. Monkman, P. Adams, Synth. Met. 40 (1991) 87–96.
[56] M.X. Wan, M. Li, J.C. Li, Z.X. Liu, J. Appl. Polym. Sci. 53 (1994) 131–139.
[57] X. Lu, Z. Wen, J. Li, Biomaterials 27 (2006) 5740–5747.
[58] D. Bouchta, N. Izaoumen, H. Zejli, M.E. Kaoutit, K.R. Temsamani, Biosen. Bioelectron. 20 (2005) 2228–2235.
[59] P. Fanjul-Bolado, D. Hernández-Santos, P.J. Lamas-Ardisana, A. Martín-Pernía, A. Costa-García, Electrochim. Acta 53 (2008) 3635–3642.
[60] R.O. Kadara, N. Jenkinson, C.E. Banks, Sens. Actuators B 138 (2009) 556–562.
[61] P. Fanjul-Bolado, P. Queipo, P.J. Lamas-Ardisana, A. Costa-García, Talanta 74 (2007) 427–433.
[62] A.J. Bard, L.R. Faulkner, Electrochemical Methods: Fundamentals and Applications, Wiley, New York, 2000, pp. 368–416.
[63] Y. Furkan, C. Emre, S. Mehmet, B. Abdulhadi, Nano-Micro Lett. 3 (2011) 91–98.
[64] M.A. Alonso-Lomillo, J.M. Kauffmann, M.J. Arcos Martinez, Biosen. Bioelectron. 18 (2003) 1165–1171.
[65] C. Lihua, L. Liuzhan, H. Shen, Chin. Sci. Bull. 50 (2005) 1834–1838.